JPNT 7(1), 1-14 (2018)
https://doi.org/10.11003/JPNT.2018.7.1.1

JPNT Journal of Positioning, Navigation, and Timing

Performance Comparison of Different GPS L-Band Dual-Frequency Signal Processing Technologies

Hyeong-Pil Kim[1], Jin-Ho Jeong[2], Jong-Hoon Won[1†]

[1]Department of Electrical Engineering, Inha University, 100 Inharo, Nam-gu, Incheon 22212, South Korea
[2]DusiTech Corporation, 44-15 Techno 10 Rd, Yuseong-gu, Daejeon 34027, South Korea

ABSTRACT

The Global Positioning System (GPS) provides more accurate positioning estimation performance by processing L1 and L2 signals simultaneously through dual frequency signal processing technology at the L-band rather than using only L1 signal. However, if anti-spoofing (AS) mode is run at the GPS, the precision (P) code in L2 signal is encrypted to Y code (or P(Y) code). Thus, dual frequency signal processing can be done only when the effect of P(Y) code is eliminated through the L2 signal processing technology. To do this, a codeless technique or semi-codeless technique that can acquire phase measurement information of L2 signal without information about W code should be employed. In this regard, this paper implements L2 signal processing technology where two typical codeless techniques and four typical semi-codeless techniques of previous studies are applied and compares their performances to discuss the optimal technique selection according to implementation environments and constraints.

Keywords: dual-frequency signal processing technology, P(Y) code, codeless, semi-codeless

1. INTRODUCTION

The signal processing technology based on dual frequency has been used to provide accurate positioning performance by analyzing measurement information between L1 and L2 signals in various fields such as earth science, urban engineering, and precision agriculture. In particular, the use of phase information of L1 and L2 signals obtained through the dual frequency signal processing technology can reduce integer ambiguity that affects the range error between satellite and receiver during positioning to provide more accurate receiver position information in fields where high precision positioning is required (Kaplan & Hegarty 2006, El-naggar 2011).

The Global Positioning System (GPS), which was deployed completely up until today, employs L1 signal whose center frequency is 1,575.42 MHz and L2 signal whose center frequency is 1,227.6 MHz largely. In L1 signal, the coarse and acquisition (C/A) code and precision (P) code are modulated and in L2 signal, the P code is modulated. The P code is a basis of the precise positioning system, which provides better positioning performance than the C/A code does. Thus, it is mainly used for military purposes. If the anti-spoofing (AS) mode applied to block a spoofing attack that disturbs signals is run in the GPS, the P code is encrypted to the Y code (or P(Y) code) through the modulation of the W code. Since only authorized users can know the secret of the W code, general users have to employ a 'codeless technique' or 'semi-codeless technique' in order to acquire the phase measurement information of L2 signal without information about the W code (Kaplan & Hegarty 2006).

A number of techniques have been proposed through various studies (Hofmann-Wellenhof et al. 1994, Woo 2000). Two of the typical codeless techniques are 'L2 squaring' that removes the effect of the P(Y) code by squaring L2 signal and 'Cross-correlation' that utilizes the P(Y) code modulated with regard to L1 signal for L2 signal processing. The codeless technique is a type that performs signal tracking even if performance is degraded to some

Received Dec 29, 2017 **Revised** Jan 31, 2018 **Accepted** Feb 05, 2018
†**Corresponding Author**
E-mail: jh.won@inha.ac.kr
Tel: +82-32-860-7406 Fax: +82-32-863-5822

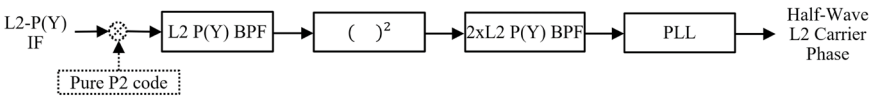

Fig. 1. L2 Squaring technique with P code aiding (dotted line) block diagram.

extent without code information. In contrast, the semi-codeless technique is a type that performs signal tracking while preventing performance degradation to some extent by using the P code which is not encrypted. Typically, four methods have been proposed: the 'P code aided L2 squaring', 'P code aided cross-correlation' 'Z-tracking' that adds the W-rate Integration & Dump processing procedure, and 'L2 Demodulation by Maximum A Posteriori (MAP)' that estimates L2 signal phase based on the maximum a posteriori theory (Woo 2000).

The present study aims to develop a simulator in which the aforementioned six L2 signal processing techniques are applied, to acquire phase information of L2 signal even in situations where the W code is not known. To do this, this study implements the P(Y) code first by generating arbitrary W code, and generates L1 and L2 signals that correspond to 32 satellites. Then, performances are analyzed by depicting a trend of change in output signals of L2 in-phase & quadrature-phase, phase error, doppler and doppler error over time. The criterion that compares the performance of signal processing of the techniques is determined by the size of Root-Mean-Square (RMS) phase error for each technique according to changes in L2 C/N_0 value. Finally, theoretical values of the RMS phase errors, which are obtained by linear approximation of the operation of phase-locked-loop (PLL) are compared to simulation values and the results are analyzed. In addition, implementation environments and constraints of all techniques implemented in this study are discussed.

2. GPS L1 & L2 SIGNAL STRUCTURE AND L2 SIGNAL PROCESSING TECHNOLOGY

2.1 Structure of GPS L1 & L2 Signals

As mentioned in the above, the C/A code and P code are modulated in GPS L1 signals, and only the P code is modulated in L2 signals. The C/A code has a chipping rate of 1.023×10^6 chips/s and 1ms cycle, and the P code has a chipping rate of 10.23×10^6 chips/s and seven days of cycle. The P(Y) code, which is the P code encrypted with the W code, has been known to have a cycle of 256 days or longer (Kaplan & Hegarty 2006).

The Intermediate Frequency (IF) received signal structure of the dual frequency GPS receiver is expressed in Eq. (1) (Jung et al. 2003).

$$\begin{aligned} r(n) = {} & A_{ca}(n)C[nT_s-\tau_1(n)]D[nT_s-\tau_1(n)]\cos[2\pi(f_{IF1}+f_{d1})nT_s+\varphi_1(n)] \\ & -A_{p1}(n)P[nT_s-\tau_1(n)]W[nT_s-\tau_1(n)]D[nT_s-\tau_1(n)]\sin[2\pi(f_{IF1}+f_{d1})nT_s+\varphi_1(n)] \\ & +A_{p2}(n)P[nT_s-\tau_2(n)]W[nT_s-\tau_2(n)]D[nT_s-\tau_2(n)]\cos[2\pi(f_{IF2}+f_{d2})nT_s \\ & +\varphi_2(n)]+\mu_{IF}(n) \end{aligned} \quad (1)$$

where r(n) is the front-end's output signal, A_{ca}, A_{p1}, and A_{p2} are the amplitude of L1 C/A, P(Y), and L2 P(Y) carrier, respectively, C is C/A code, P is the known P code, W is the encrypted W code, D is the 50 bps navigation data bit stream, τ_1 and τ_2 are the code phase of L1 and L2, respectively, f_{IF1} and f_{IF2} are the IF of L1 and L2, respectively, f_{d1} and f_{d2} are the doppler of L1 and L2, respectively, φ_1 and φ_2 are the carrier phase of L1 and L2, respectively, and μ_{IF} is zero-mean discrete time Gaussian noise.

As presented in Eq. (1), the P code is encrypted due to the W code. The L1-P(Y) code has a quadrature-phase offset whereas the L2-P(Y) code has an in-phase offset. Thus, the P(Y) code phase obtained from the L1 tracking loop implies that it can help to find the appropriate alignment status of the L2-P(Y) code and carrier phase.

2.2 L2 Codeless Techniques

The L2 codeless techniques applied to this study are two folds: L2 squaring and cross-correlation.

2.2.1 L2 squaring

This technique squares signals to remove the effect of the P(Y) code in L2 signals, and consists of two band pass filters (bandwidths are approximately 20 MHz and 40 MHz) that pass the P(Y) code frequency band and one phase locked loop. The signal processing procedure is shown in the solid line in Fig. 1. Since signals were squared, L2 carrier waves whose center frequency becomes twice are produced. However, since a wavelength of the output signal is reduced by half accordingly, the integer ambiguity problem between satellite and receiver, which has been an issue in geodetic survey applications in particular, is increased. In addition, as a bandwidth of L2 signals becomes wider due to the signal squaring, the noise effect becomes larger thereby degrading the SNR performance, which has been a problem

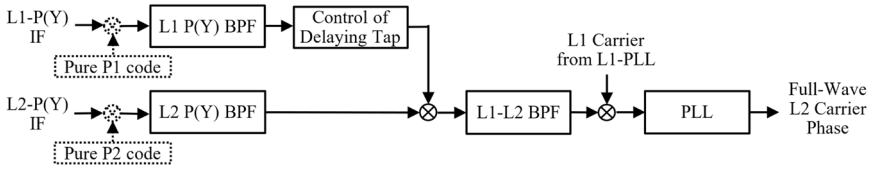

Fig. 2. Cross-correlation technique with P code aiding (dotted line) block diagram.

(Ashjaee et al. 1990, Woo 2000).

2.2.2 Cross-correlation

This technique eliminates the effect of the P(Y) code by multiplying L2 signal by L1 signal, and consists of three band pass filters (two filters whose bandwidth is approximately 20 MHz and one filter whose center frequency is L1-L2) and one phase locked loop. The solid line in Fig. 2 shows the operation process. When L1 and L2 signals that are transmitted from satellites pass through the ionosphere, these two signals are refracted depending on the center frequency. Thus, the L1 signal is appropriately delayed through the delaying tap and then the code is aligned with the L2 signal to eliminate the P(Y) code. The L1-L2 signal whose center frequency is the product of two signals is produced, and this signal is multiplied by L1 signal that is restored through code correlation with the C/A code to recover the center frequency of L2 signal thereby obtaining the L2 signal phase information of the full wavelength (MacDoran et al. 1984).

The accuracy of the delaying tap in the cross-correlation is dependent on a sampling rate. Thus, if a sampling resolution is larger than an amount of phase mismatch between L1 and L2, the SNR performance is degraded. It has also a wide bandwidth problem of the passed noise since the L1 and L2 signals are multiplied in a wide range of bandwidth (Woo 2000).

2.3 L2 Semi-codeless Techniques

In general, the semi-codeless techniques show better SNR performance than that of the codeless techniques because they remove the effect of the P code at the input layer in priority using the P replica code. This study applied the aforementioned four techniques.

2.3.1 P code aided L2 squaring

This technique improved the L2 squaring technique. In this technique, the effect of the P code is eliminated from the input layer so that only the effect of the W code in the P(Y) code is processed. Thus, two band pass filters have approximately 1 MHz and 2 MHz bandwidths that are passed through the W code frequency band so that the effect of the noise is significantly reduced. The drawback of this technique is that integer ambiguity is increased due to the wavelength of the output signal that is reduced by half as explained in the L2 squaring technique. Fig. 1 shows the operation process with solid and dotted lines (Keegan 1990, Woo 2000).

2.3.2 P code aided cross-correlation

This technique improved the cross-correlation technique. In this technique, the effect of the P code is eliminated from the input layer so that only the effect of the W code in the P(Y) code is processed with a narrow signal bandwidth. Fig. 2 shows the operation process with solid and dotted lines. It can obtain the advantages of the cross-correlation technique and P code aiding method simultaneously. Its performance is comparable with the Z-tracking technique, which is explained in the next, but the implementation is simpler. The drawback of this technique is similar to that of the cross-correlation technique (Woo 2000).

2.3.3 Z-tracking

This technique employs timing information obtained through the relationship between P code and W code along with the application of the P code aiding method. Fig. 3 shows the signal processing procedure. The W code has a timing relationship with X1A code generator used to generate the P code, and the chip duration of the W code can be aligned with around 20 P code chips. Thus, the transition point of the W code can be found via search of the maximum signal power through the W-rate integration & dump (I&D) filter located in the L1 and L2 signal path. Through this, L1 signal is multiplied with L2 signal to remove the effect of the W code and the phase information of the full-wave L2 signal can be obtained through the operation of the phase locked loop (Lorenz et al. 1992).

The signal's bandwidth is reduced using the P code aiding method, and the effect of the W code can be eliminated in

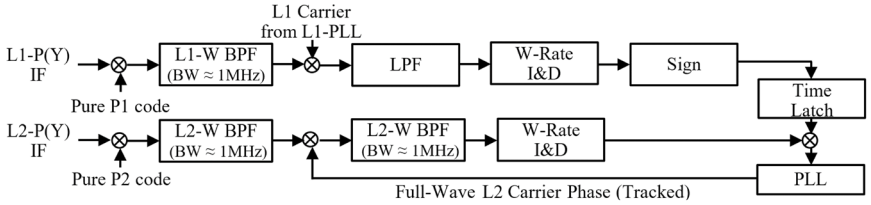

Fig. 3. Z-tracking technique block diagram.

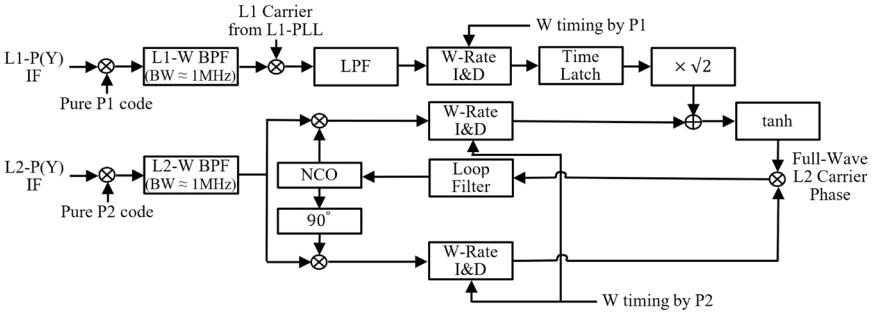

Fig. 4. L2 demodulation by MAP technique block diagram.

a narrow bandwidth by estimating the W code through the W-rate I&D filter. Accordingly, the Z-tracking technique provides better signal processing performance than that of the aforementioned codeless techniques. However, this technique has the following shortcomings that the bit estimation of the W code is based on a simple method using the sign of L1 signal, and its implementation is more complex than the aforementioned techniques because of using multiple filters (Woo 2000).

2.3.4 L2 demodulation by MAP

Although this technique is based on the Z-tracking, it can provide better signal processing performance by using the Costas loop that can reduce uncertainties of the W chip duration and MAP estimator, which can find more accurate L2 signal phase information considering the combination of the L1 and L2 signals (Simon & Lindsey 1977). The operation procedure is shown in Fig. 4. Since the MAP estimation theory is applied, the optimal L2 signal phase estimator can be obtained by finding the L2 signal phase that can maximize the joint probability density function of three baseband signals, which are the outcome passed through the P code aiding operation when the W-bit data are random (Woo 2000, Woo et al. 2000).

The structure of the semi-codeless technique through the MAP estimator is more complex and has more computational load than other techniques. The squaring loss in the approximate MAP and MAP estimator used technique according to changes in L2 C/N_0 did not show a significant difference in the linearly approximated theoretical value (Woo 2000). Thus, the simulation of this study reduced the computational load by applying the linearized MAP estimator, in which tanh(x) was approximated to x.

3. DEVELOPMENT OF SIMULATOR OF GPS L–BAND DUAL FREQUENCY SIGNAL PROCESSING TECHNIQUES

3.1 Signal Generation

Since L1 signal includes C/A code, P code, and W code, and L2 signal includes P code and W code as presented in Eq. (1), code for a single satellite is first generated. In addition, the main code is made by applying the pseudo random noise (PRN) number that can help us to distinguish a total of 32 GPS satellites to the code according to the appropriate shift. Finally, parameters such as phase or frequency are set up to generate main code-applied L1 & L2 signals.

For the C/A code generation method, the following reference was used (Kaplan & Hegarty 2006). In the simulator, the PRN number shift about 32 GPS satellites are applied to the G2 register output of the code generator, which is then modulo-2 operated with the G1 register output.

For the P code generation method, CGSIC (2013) was referred. A length of one-cycle P code is very long, which

Table 1. Parameters of simulator.

Simulation parameters	Simulation values	Notes
Simulation time	30 seconds (running in 0 to 30)	User defined
L1-IF, L2-IF signal frequency	20.26 MHz, 28.12 MHz	
Chipping-rate of C/A, P, W code	1.023 MHz, 10.23MHz, 511.5 KHz	
Sampling frequency	81.84 MHz	User defined
Carrier Loop Noise Bandwidth	5 Hz	User defined
C/N_0 range	24 to 52 dB-Hz • 4 dB-Hz intervals • RF front-end noise bandwidth: 40 MHz	User defined
L2 Doppler profile	15 to 75 Hz for 30 seconds • Initial L2 Doppler offset: 15Hz • Doppler rate: 2 Hz/s (increasing)	User defined
Assumption	• Doppler offset difference between L1 and L2: 3 Hz • Power ratio of L1/L2: 2 • Alignment of L1-P and L2-P code • W code is aligned with P code	
Simulation Tool	MATLAB R2017a	

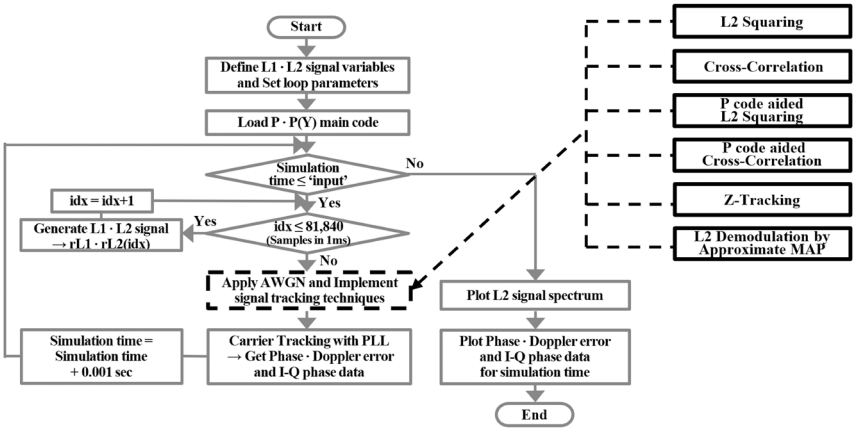

Fig. 5. Flow-chart of simulator operation with 6 techniques.

can induce a significant computation load on the simulator. Thus, the simulator generates arbitrary P code epoch whose time period is 1.5 sec. and code period is 15,345,000 chips by multiplying X1 and X2 code, and it applies a shift to the satellite PRN number.

To generate the P(Y) code, the W code is needed. The chipping rate of the W code is set to 511.5 kHz, which is 1/20 times of that of the P code, and the W code which has an arbitrary value ranged between 1 and -1 is generated by using the *randi* function in MATLAB (Borio 2011). This is multiplied with the P code to generate the P(Y) code of 1.5 sec. long (=15,345,000 chips). A total of 32 arrays of P code and P(Y) code are stored by applying the PRN offset delay of 32 GPS satellites to the generated P code and P(Y) code. These data are used to generate L2 signals or implement the simulator of L2 signal processing techniques.

The parameter setup values of the simulator developed to generate and process L2 signals are presented in Table 1. A sampling frequency is set to 81.84 MHz to implement L2 discrete signal within the receiver. Thus, when a total simulation time is 1.5 sec, a total of 122,760,000 (=1.5 × 81,840,000) samples are acquired. Then, L2 signals are generated by substituting the previously generated P(Y) code to the samples appropriately. For the P(Y) code, satellites whose PRN number is one in the main code are employed.

3.2 Signal Processor

3.2.1 Application of L2 codeless techniques

Fig. 5 shows a flow chart of the L2 squaring-applied simulator operation. The overall structures of the aforementioned six techniques are all the same. A time required for a single block is set to 0.001 sec. and it is iterated by 30,000 times to satisfy 30 sec. of the simulation time. Furthermore, smaller block within the 0.001 sec. block are iterated by 81,840 times to satisfy the sampling frequency 81.84 MHz. The white Gaussian noise is added to L2 signals that are sampled to 81,840 samples in each block and the squaring technique is applied. The discriminator

of the PLL is implemented by applying the arctangent function to the quadrature-phase punctual signal divided by the in-phase punctual signal, and the 3rd order loop-filter is selected. The phase error of the simulator is reduced gradually by producing the next-step phase, doppler, and current phase error information through the PLL, and L2 signals are tracked through the above process. As the simulation is terminated, the simulator operation is finished with making a diagram of change trend of phase error, doppler frequency, doppler error, and in-phase & quadrature-phase outputs of L2 signal over time.

When the cross-correlation technique is applied, L1 signal whose initial doppler is 12 Hz, L1 signal band pass filter, and a band pass filter, which has the L1-L2 center frequency, are added compared to the L2 squaring technique. The L1-L2 filter output is restored to the L2 center frequency signal by multiplying the carrier wave of L1 signal which has an initial doppler value. In addition, a delaying tap is implemented assuming that a difference in refractive index in the ionosphere between L1 and L2 signals is compensated. This assumption is also applied to other techniques.

3.2.2 Application of L2 semi-codeless techniques

In the simulator where the P code aided L2 squaring technique is applied, signals are sampled to 81,840 samples as the same as done in the L2 squaring technique, and then multiplied with the sampling P replica code to eliminate the effect of the P code. Since the signal bandwidth is reduced by 1/20 times through this operation, the band pass filter is implemented to have a bandwidth of 1 MHz and 2 MHz.

When the P code aided cross-correlation technique is applied, the signal is multiplied by P replica code to eliminate the effect of the P code first in addition to the cross-correlation technique. Accordingly, the band pass filter is implemented to have a bandwidth reduced by 1/20 times.

When the Z-tracking technique is applied, the effect of the P code is eliminated by multiplying the generated L1 and L2 signals by the P replica code prior to processing with the W-rate band pass filter. In addition, a low-pass filter of around 1 MHz of bandwidth is added to filter the L1 recovery signal in the L1 signal path.

In this simulator, a variable called *dump* is also generated during signal generation to apply the W-rate I&D filter. A point where the *dump* becomes one is a transition point, which can help finding the cycle of the W code. Furthermore, a variable called *matdump* is used so that the sign of total sum which adds all L1 recovery signal codes stored between two *dump* which becomes one is substituted with variable called *IandDL*1. This is an output of the L1 signal path and L2 signal is also produced through the W-rate I&D. Then, the L2 signal tracking through the PLL is implemented after L1 output signal is multiplied with L2 output signal.

In the simulator where the L2 demodulation by approximate MAP is applied, Z-tracking and variables, parameters, and filters are the same but a total sum of signal code stored between two *dump* which becomes one is used instead of using the sign of total sum when *landDL*1 signal is generated. In addition, the Costas loop is implemented as a PLL. Variable *mapL*1 generated inside the PLL is not only an output of the W-rate I&D filter in the L1 signal path but also *landDL*1 signal, which is an input of the PLL. Furthermore, variable *preIDI* is L2 in-phase signal after passing through the W-rate I&D filter in the Costas loop, and variable *mapIDQ* is L2 quadrature-phase signal after passing through the filter. Thus, the MAP technique that applies the addition of *mapL*1 and *preIDI* to the *tanh* function is implemented, and this output signal and *mapIDQ* are multiplied and feed-backed to perform L2 signal tracking.

In this study, approximate MAP technique which approximates the *tanh* function linearly is employed rather than using the MAP technique.

4. RESULTS OF PERFORMANCE TESTS OF GPS L-BAND DUAL FREQUENCY SIGNAL PROCESSING TECHNIQUES

The simulation results of the simulator where each of the techniques are applied are presented with diagrams of changes in L2 in-phase & quadrature-phase output signals, phase error, doppler, and doppler error over time. First, results of six simulators when C/N_0 value is 24 dB-Hz and 52 dB-Hz are compared assuming extreme receive signal environments to verify the availability of L2 signal tracking function for each technique. Second, the RMS phase error results according to various C/N_0 values are summarized and compared with theoretical values of the RMS phase error obtained by linearly approximated results of PLL operation to analyze the tracking performance of each technique. Finally, advantages and disadvantages of each technique are compared through the trade-off analysis.

4.1 Availability Test

The results of L2 squaring technique are shown in Figs. 6 and 7. As shown in Fig. 6, when C/N_0 is 24 dB-Hz, a phase error of L2 signal is large and a doppler error cannot become zero

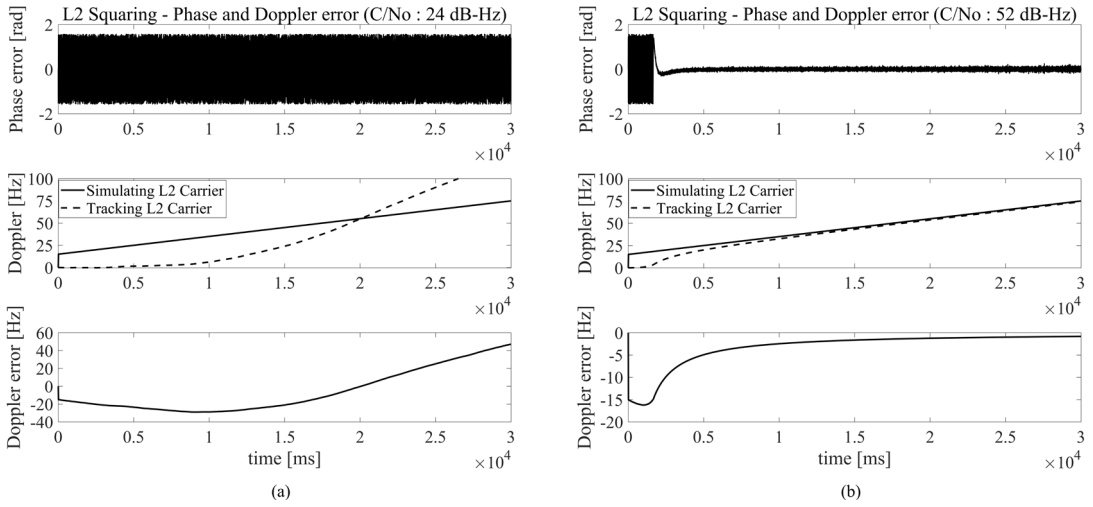

Fig. 6. Phase error, doppler, doppler error change of L2 squaring technique over 30 seconds. (a) C/N_0 : 24 dB-Hz (b) C/N_0 : 52 dB-Hz

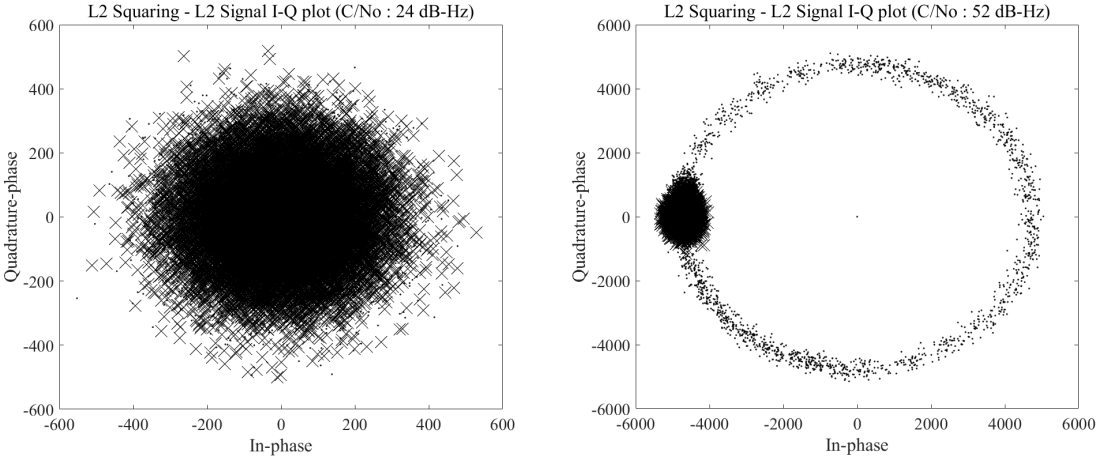

Fig. 7. In-phase and quadrature-phase L2 signal plot of L2 squaring technique. (a) C/N_0 : 24 dB-Hz, (b) C/N_0 : 52 dB-Hz

even if time passes. In contrast, when C/N_0 value is 52 dB-Hz, a phase error and doppler error are converged close to zero, and tracking L2 carrier reduces a doppler error and tracks the simulating L2 carrier graph well, which is set in the simulator. Subsequently, in Fig. 7, as a phase error is converged close to zero, a value of sum of in-phase and quadrature-phase signal vectors should be presented over the I-axis in the I-Q plane. To verify whether the phase error is converged or not, the time reference point is set to 10 sec. Afterward, the I-Q plot is set to be depicted with X-shape symbol, which has I and Q correlation values as a plane coordinate. When C/N_0value is 24 dB-Hz, variances of the I and Q correlation values are very large. Thus, X symbols are dispersed. However, for 52 dB-Hz, X symbols are converged close to the I-axis.

The results of cross-correlation technique are shown in Figs. 8 and 9a. When C/N_0 is 24 dB-Hz, a doppler error continues to increase and it verifies that signal tracking is not performed well. Furthermore, when C/N_0 value is 52 dB-Hz, RMS phase error values with regard to a range of simulation time 10 to 30 sec. is 2.39 degree. Thus, its phase error due to L2 signal tracking is smaller than that of L2 squaring technique which has 2.79 degree of resulting value.

The results of P code aided L2 squaring technique are shown in Figs. 10 and 9b. When C/N_0 is 24 dB-Hz, signals are not tracked but when C/N_0 value is 52 dB-Hz, a smaller correlation variance than that of L2 squaring technique in the I-Q plot is verified.

The results of P code aided cross-correlation technique are shown in Figs. 11 and 12a. When C/N_0 is 24 dB-Hz, signals are not tracked but when C/N_0 value is 52 dB-Hz, a smaller correlation variance than that of cross-correlation technique in the I-Q plot is verified.

The results of Z-tracking technique are shown in Figs. 13

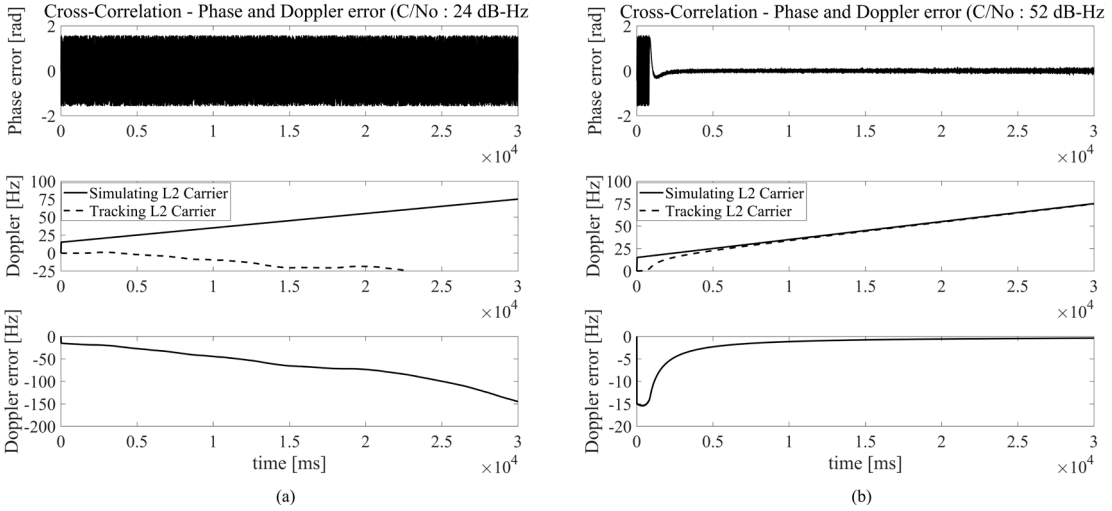

Fig. 8. Phase error, doppler, doppler error change of cross-correlation technique over 30 seconds. (a) C/N_0 : 24 dB-Hz (b) C/N_0 : 52 dB-Hz

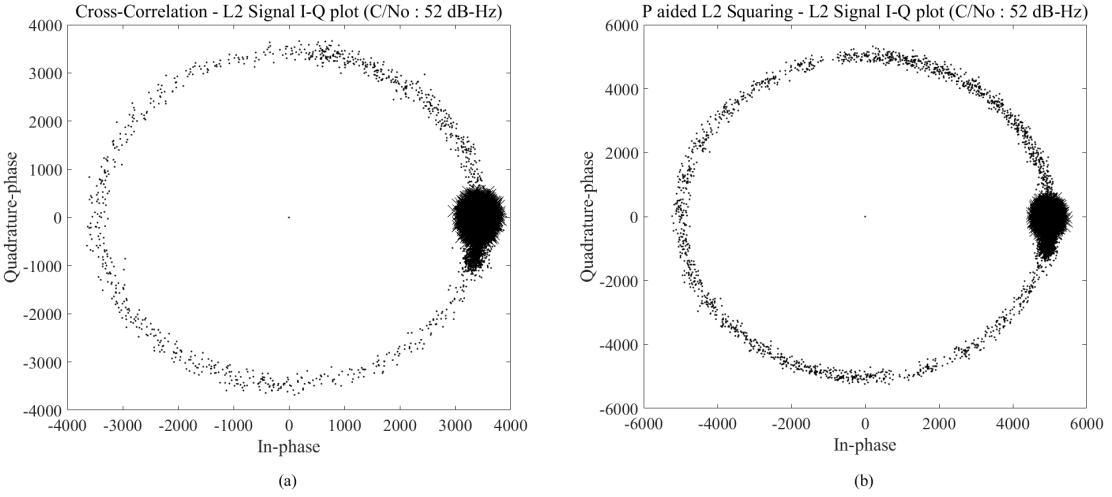

Fig. 9. In-phase and quadrature-phase L2 signal plot, when C/N_0 : 52 dB-Hz. (a) Cross-correlation, (b) P aided L2 squaring

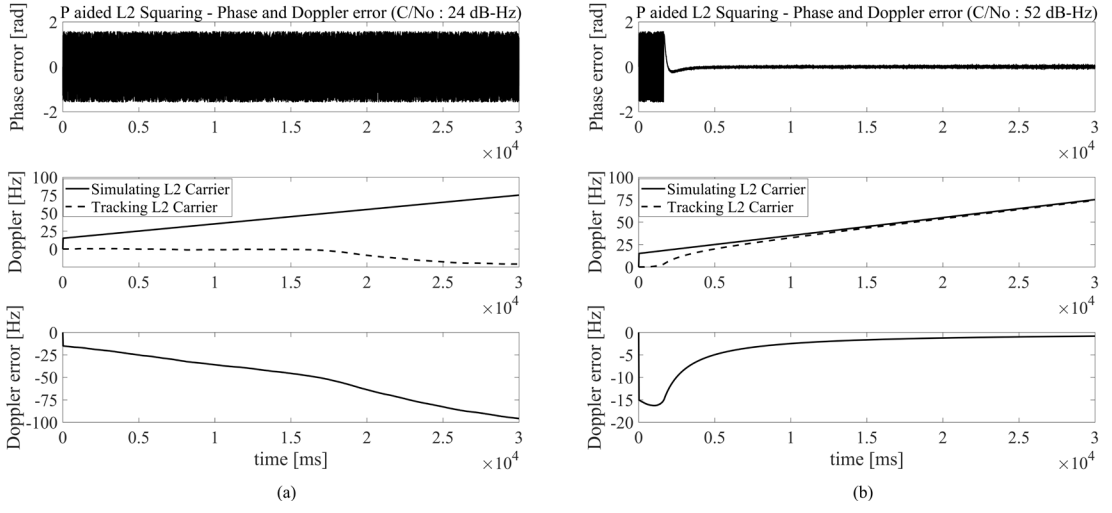

Fig. 10. Phase error, doppler, doppler error change of P code aided L2 squaring technique over 30 seconds. (a) C/N_0 : 24 dB-Hz, (b) C/N_0 : 52 dB-Hz

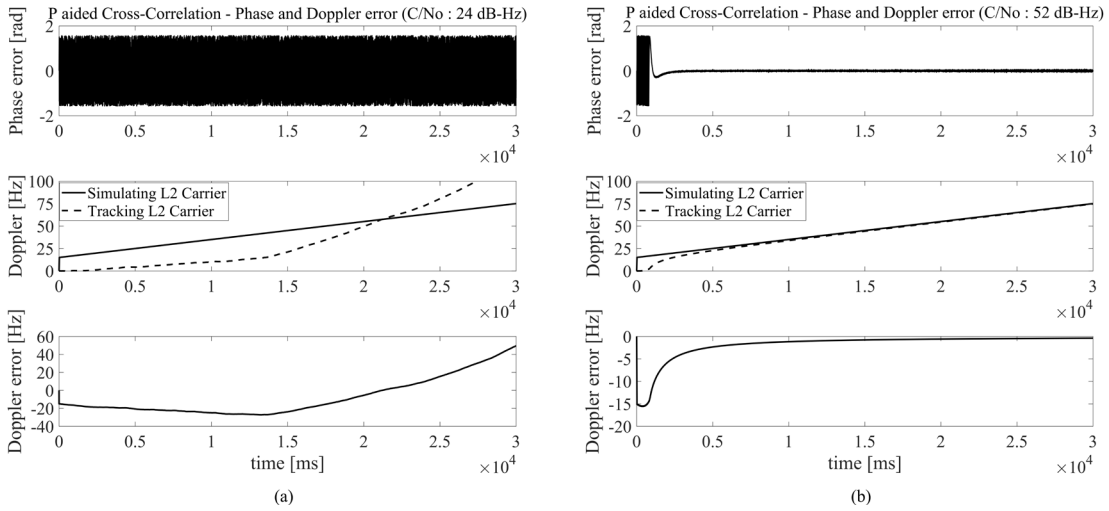

Fig. 11. Phase error, doppler, doppler error change of P code aided cross-correlation technique over 30 seconds. (a) C/N_0 : 24 dB-Hz (b) C/N_0 : 52 dB-Hz

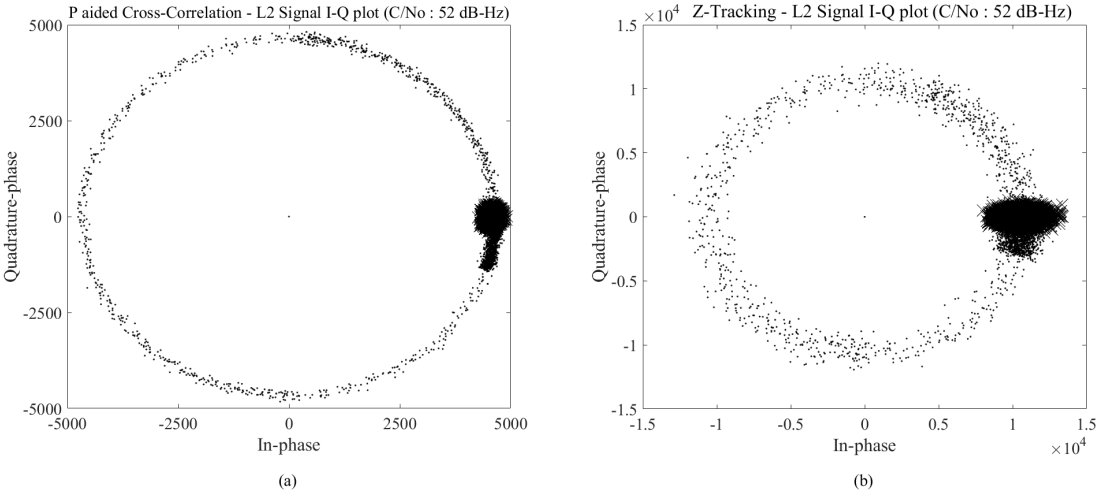

Fig. 12. In-phase and quadrature-phase L2 signal plot, when C/N_0 : 52 dB-Hz. (a) P aided cross-correlation, (b) Z-tracking

and 12b. As C/N_0 value is higher, the simulator can track L2 signals better. The I-Q plot in Fig. 12b shows that a variance of correlation values is slightly larger than that of previous techniques when L2 signals are tracked, which is because the W code that has a value of 1 and -1 arbitrarily is passed through the I&D filter.

The results of the L2 demodulation by approximate MAP technique are shown in Figs. 14 and 15. As shown in Fig. 14, a phase error and doppler error are decreased even C/N_0 value is lower in contrast with those in the previous techniques, which exhibits a trend of L2 signal tracking to some extent. Fig. 15 shows that when C/N_0 value is 52 dB-Hz, the I-Q plot is deviated to the right side in the I axis. This is because the addition of L1 signal and L2 in-phase signal are considered as the in-phase value in the I-Q plot in the procedure of L2 signal separation processing. The L1 signal has a positive bias value after passing through the W-rate I&D filter, and the size of the bias is increased proportionally with the C/N_0 value. This is added to the L2 in-phase signals according to the MAP technique operation process so that the I-Q plot is biased to the positive direction. In addition, I correlation value becomes large as shown in Z-tracking. This is revealed due to the combined effects of the W code whose value is 1 and -1 arbitrarily after passing through the I&D filter and the aforementioned L1 signal bias. Most of the X symbols are presented over the I-axis, which satisfies the condition of L2 signal tracking.

4.2 Sensitivity Test

The theoretical value of the RMS phase error and simulator operation results by technique used according to C/N_0 value

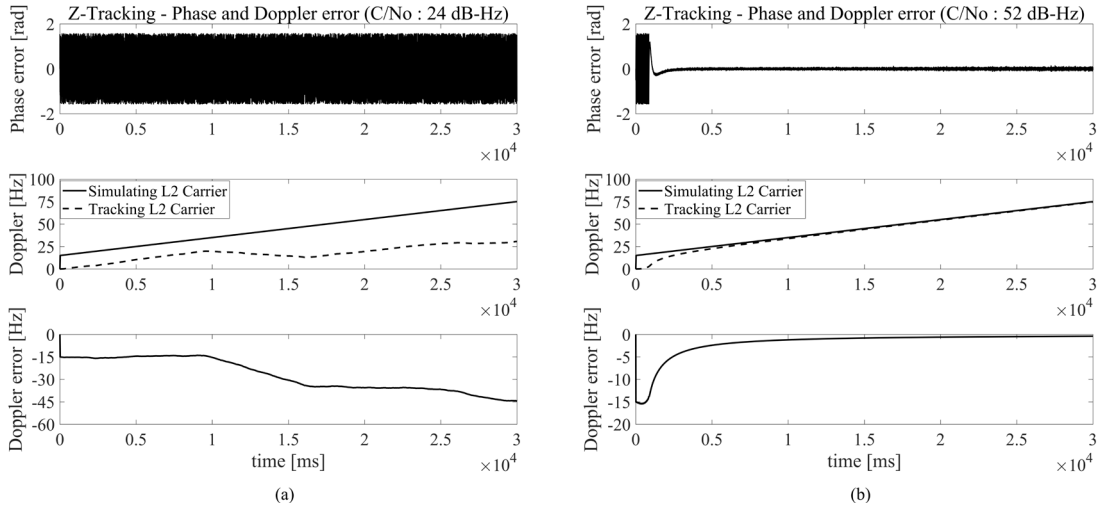

Fig. 13. Phase error, doppler, doppler error change of Z-tracking technique over 30 seconds. (a) C/N_0 : 24 dB-Hz, (b) C/N_0 : 52 dB-Hz

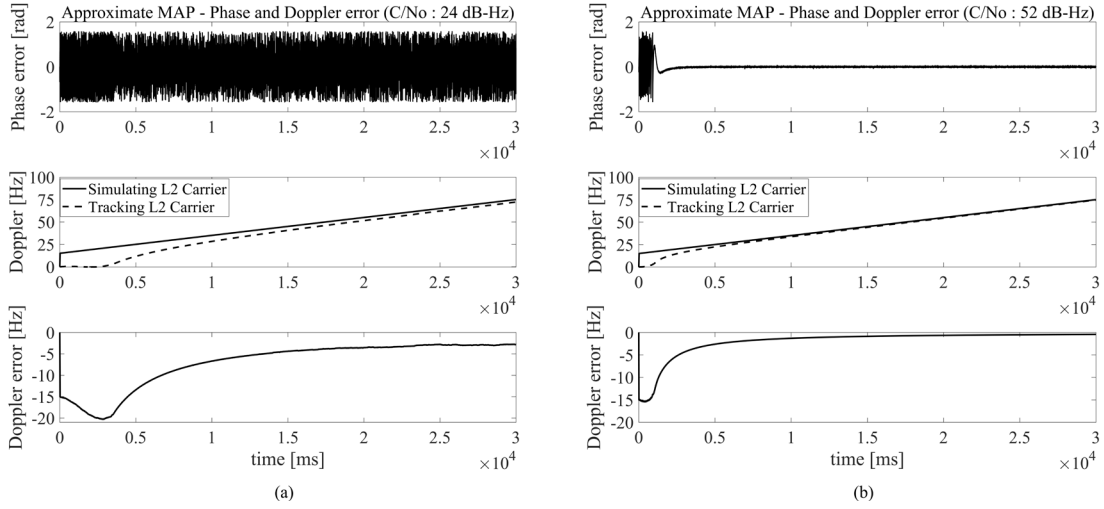

Fig. 14. Phase error, doppler, doppler error change of L2 demodulation by approximate MAP Technique over 30 seconds. (a) C/N_0 : 24 dB-Hz, (b) C/N_0 : 52 dB-Hz

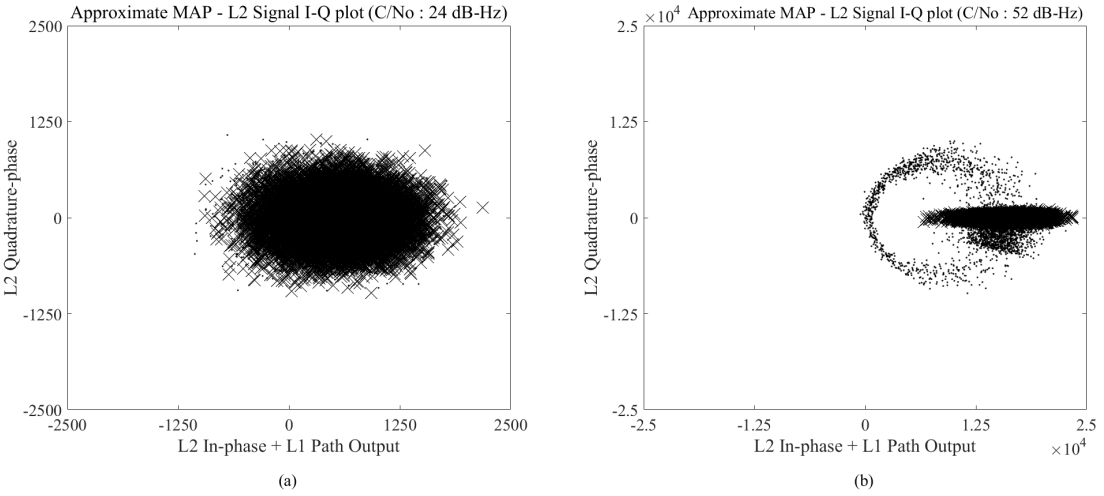

Fig. 15. In-phase and quadrature-phase L2 signal plot of L2 demodulation by approximate MAP technique. (a) C/N_0 : 24 dB-Hz, (b) C/N_0 : 52 dB-Hz

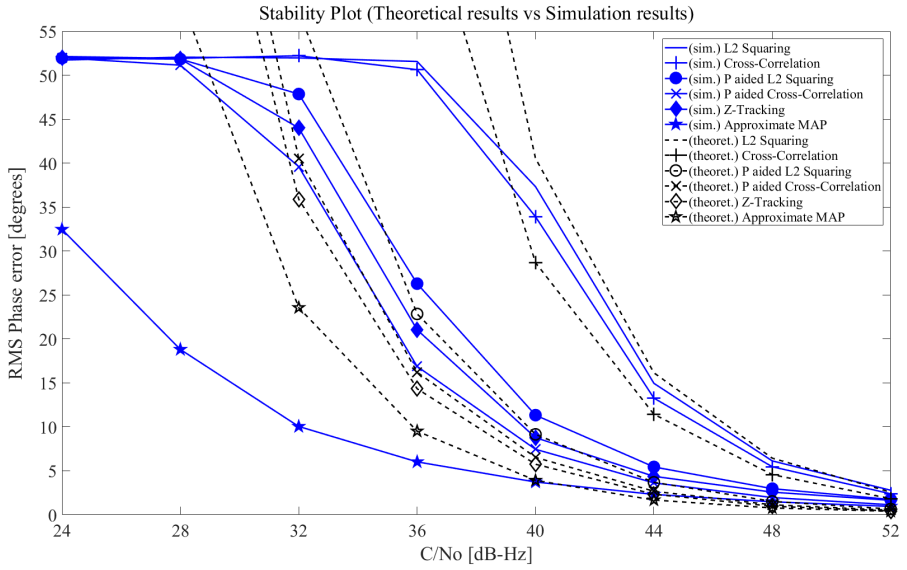

Fig. 16. Stability plot of 2 codeless and 4 semi-codeless techniques (solid line: simulation result, dotted line: theoretical result).

are depicted with dotted and solid lines, respectively, which are shown in the stability plot of Fig. 16. The equation that induces the theoretical values is presented in Eq. (2), and the signal tracking loop bandwidth of the parameter required for calculation is set to 5 Hz as same as that of the simulator. The equations that calculate a squaring loss for each technique are summarized in Table 2 (Woo 2000).

$$\sigma_{\emptyset}{}^{2} = \left[\frac{C}{N_0 B_L} S_L\right]^{-1} \tag{2}$$

where $\sigma_{\emptyset}$ is the RMS phase error of the tracking loop, C/N_0 is the received carrier to noise power spectral density ratio, B_L is the loop bandwidth, and S_L is the squaring loss factor.

The actual simulation results exhibit a certain level of bias of C/N_0 values. Thus, a trend of the theoretical values and simulation result values are compared and analyzed after subtracting bias collectively. When two values are compared, the order of improvements on signal tracking performance is nearly the same as the techniques become advanced. However, the simulation result values show that the Z-tracking technique is degraded more than the P code aided cross-correlation technique in contrast with the theoretical values. This implies that precise computation required in the W-rate I&D filtering procedure that estimates a cycle of the W code has some problem compared to the cross-correlation technique that removes the effect of the P code and W code simply using the product of L1 and L2 signals. In addition, the approximate MAP technique-applied results show lower phase errors than those of the theoretical values in a range of low C/N_0 values. This is due to the presence of limit value of RMS phase errors for every technique in actual simulations so that phase errors are increased at a lower rate rather than that of theoretical values which have no limits. The techniques have limit values of 52 degree approximately.

Table 2. Summary of squaring loss formulas (Woo 2000).

Technique	Squaring loss for L2 demodulation
L2 squaring	$S_L \cong \frac{1}{1+\frac{B_P}{2C/N_0}}$, $B_P \approx 20\ MHz$
Cross-correlation	$S_L \cong \frac{1}{1+\frac{B_P}{4C/N_0}}$, $B_P \approx 20\ MHz$
P code aided L2 squaring	$S_L \cong \frac{1}{1+\frac{B_W}{2C/N_0}}$, $B_W \approx 1\ MHz$
P code aided cross-correlation	$S_L \cong \frac{1}{1+\frac{B_W}{4C/N_0}}$, $B_W \approx 1\ MHz$
Z-tracking	$S_L \cong erf^2\sqrt{2T_W\ C/N_0}$, $T_W \approx 2\ \mu sec$
Approximate MAP	$S_L \cong \frac{1}{1+\frac{1}{6T_W\ C/N_0}}$, $T_W \approx 2\ \mu sec$

Table 3 presents simulation values of the RMS phase errors according to C/N_0 value in a range of 24 dB-Hz to 52 dB-Hz as shown in Fig. 16 divided by technique. The table

Table 3. RMS phase error value [degree] of 6 techniques.

C/N_0 [dB-Hz]	Technique					
	L2 squaring	Cross-correlation	P code aided L2 squaring	P code aided cross-correlation	Z-tracking	Approximate MAP
24	51.72	52.12	51.94	51.97	52.00	32.46
28	52.05	51.92	51.83	51.14	51.84	18.81
32	51.96	52.21	47.85	39.59	44.00	10.05
36	51.56	50.63	26.29	16.87	21.04	6.02
40	37.32	33.90	11.33	7.45	8.77	3.73
44	14.96	13.27	5.44	3.63	4.37	2.32
48	6.13	5.46	2.97	1.96	2.58	1.48
52	2.79	2.39	1.74	1.14	1.65	0.96

Table 4. Trade-off analysis for 6 techniques.

Technique	Characteristic	Implementation complexity (Compared to L2 Squaring)	Squaring loss [dB] (at 40 dB-Hz)
L2 squaring	• Simple operation and easy implementation • Double doppler error • Wide bandwidth BPF • Half-wavelength L2 output	-	-30
Cross-correlation	• Use L1 signal to remove P(Y) code effect • Wide & L1-L2 bandwidth BPF • Full-wavelength L2 output	it requires: • L1 signal & carrier • Control of delaying tap	-27
P code aided L2 squaring	• Narrow bandwidth BPF • Double doppler error • Half-wavelength L2 output	it requires: • P code aiding	-17
P code aided cross-correlation	• Use L1 signal to remove W code effect • Narrow bandwidth BPF • Full-wavelength L2 output	it requires: • P code aiding • L1 signal & Carrier • Control of delaying tap	-14
Z-tracking	• Use L1 signal to remove W code effect • Narrow bandwidth BPF • Use timing information between P & W code • Estimate W code bit by using sign	it requires: • P code aiding • L1 signal & Carrier • W-Rate I&D filter • Time Latch	-13
Approximate MAP	• The best L2 tracking performance • Use timing information between P & W code • Get optimal L2 phase by using MAP estimator • Has a little more computational burden than other techniques	it requires: • P code aiding • L1 signal & carrier • W-Rate I&D filter • Time Latch • Costas Loop & MAP estimator	-10

verifies that when 15 degree is considered as the L2 signal tracking threshold, signal tracking can be possible even in a low C/N_0 value as the technique becomes advanced.

As a result, when the L2 demodulation by approximate MAP technique is applied to the simulator, it shows the smallest RMS phase error values in the same C/N_0 value, which has the best signal processing performance, verifying that the trends of theoretical and test results in signal processing performance for each technique are nearly matched.

4.3 Trade-off Analysis

Table 4 summarizes the characteristics, implementation complexity, and theoretical values of squaring loss when L2 C/N_0 value is 40 dB-Hz of the six techniques used in this study. As the technique operation used is simpler, implementation becomes easier whereas it has a larger squaring loss and worse L2 signal tracking performance. On the contrary, as the operation used becomes complex, implementation is difficult but it provides a better performance than those of the previous techniques with a smaller squaring loss consequently.

Table 5. Real average time [second] required to simulate 6 techniques over 30 seconds.

Technique	Time required [sec]
L2 squaring	750
Cross-correlation	1,348
P code aided L2 squaring	788
P code aided cross-correlation	1,365
Z-tracking	1,407
Approximate MAP	1,418

Table 5 presents a mean value of actual time taken during 30-sec. simulation operation for each technique. The two squaring method-applied techniques take a shorter time during the simulation operation than other

techniques, which take more time because they use L1 signals. As the technique used becomes advanced, the simulation operation time taken is increased more. This result implies that squaring-applied techniques are effective for rapid signal processing operation during actual receiver implementation, and if more precise results that cannot be acquired using those techniques are needed, more advanced techniques should be applied even with sacrificing more additional time taken.

5. CONCLUSIONS

This study aimed to develop a GPS L-band dual frequency signal processing technique, which improves positioning performances. To achieve this, a L2 codeless & semi-codeless-applied simulator that acquired phase information of L2 signal, which had encrypted code, was implemented and signal processing performance of each technique was compared. The simulation results verified that the simulator was able to track L2 signals with P(Y) code well as C/N_0 value was increased, and the performance was improved further as the technique used became advanced. The signal processing performances of the six techniques used in this study were nearly matched with the corresponding theoretical results. However, when test and theoretical values will be compared in the future, some effort to improve Z-tracking performance and certain bias compensation for C/N_0 value will be needed. The summarized results of availability, sensitivity test & trade-off analysis exhibited that an appropriate signal tracking technique should be selected according to implementation environments and constraints for L2 signal processing.

ACKNOWLEDGMENTS

This paper is the result of the 'Space Core Technology Development Project' funded by the Ministry of Science and ICT [Project Number: 2015M1A3A3A03027531].

REFERENCES

Ashjaee, J., Helkey, R. J., Lorenz, R. G., & Sutherland, R. A. 1990, Global Positioning System Receiver with Improved Radio Frequency and Digital Processing, US Patent 4928106A

Borio, D. 2011, Squaring and Cross-Correlation Codeless Tracking: Analysis and Generalisation, IET Radar Sonar & Navigation, 5, 958-969. https://doi.org/10.1049/iet-rsn.2011.0235

El-naggar, A. M. 2011, Enhancing the accuracy of GPS point positioning by converting the single frequency data to dual frequency data, Alexandria Engineering Journal, 50, 237-243. https://doi.org/10.1016/j.aej.2011.03.003

Hofmann-Wellenhof, B., Lichtenegger, H., & Collins, J. 1994, Global Positioning System: Theory and Practice (Wien New York: Springer-Verlag)

Jung, H., Psiaki, M. L., & Powell, S. P. 2003, Kalman-Filter-Based Semi-Codeless Tracking of Weak Dual-Frequency GPS Signal, Proceeding of ION GPS/GNSS 2003, September 9-12, 2003, Oregon Convention Center, Portland, OR, pp.2515-2523

Kaplan, E. D. & Hegarty, C. J. 2006, Understanding GPS: Principles and Applications, 2nd ed. (Boston: Artech House Inc.)

Keegan, R. G. 1990, P-Code-Aided Global Positioning System Receiver, US Patent 4972431A

Lorenz, R. G., Helkey, R. J., & Abadi, K. K. 1992, Global Positioning System Receiver Digital Processing Technique, US Patent 5134407A

MacDoran, P. F., Miller, R. B., Buennagel, L. A., Fliegel, H. F., & Tanida, L. 1984, Codeless GPS Systems for Positioning of Offshore Platforms and 3D Seismic Surveys, Journal of The Institute of Navigation, 31, 57-69. https://doi.org/10.1002/j.2161-4296.1984.tb00862.x

Simon, M. K. & Lindsey W. C. 1977, Optimum Performance of Suppressed Carrier Receivers with Costas Loop Tracking, IEEE Transactions on Communications, 25, 215-227. https://doi.org/10.1109/TCOM.1977.1093805

The Civil Global Positioning System Service Interface Committee (CGSIC) 2013, Navstar GPS Space Segment/ Navigation User Interfaces (IS-GPS-200H)

Woo, K. T. 2000, Optimum Semi-Codeless Carrier Phase Tracking of L2, Journal of The Institute of Navigation, 47, 82-99. https://doi.org/10.1002/j.2161-4296.2000.tb00204.x

Woo, R. K. T., Quan, J. O., & Cheng, U. 2000, System and Method for Demodulating Global Positioning System Signals, US Patent 6125135

Hyeong-Pil Kim is a M.S. student in the Department of Electrical Engineering at Inha University, Korea. He received B.S. degree from Inha University in 2017. His research interests include GNSS receiver signal processing and Anti-Jamming technology.

Jin-Ho Jeong is a CEO in the Software Engineering at DusiTech co., LTD, Korea. He received the Ph.D degree in the Department of sUAV Consulting from Paichai University, Korea, in 2017. He has been working at the same company since 1998. His research interests include GNSS receiver signal processing, DGNSS reference station, Anti-Jamming technology and small UAV platform.

Jong-Hoon Won received the Ph.D degree in the Department of Control Engineering from Ajou University, Korea, in 2005. After then, he had worked with the Institute of Space Technology and Space Applications at University Federal Armed Forces (UFAF) Munich, Germany. He was nominated as Head of GNSS Laboratory in 2011 at the same institute, and involved in lectures on advanced receiver technology at Technical University of Munich (TUM) since 2009. He is currently an assistant professor of Electrical Engineering of Inha University. His research interests include GNSS signal design, receiver, navigation, target tracking systems and self-driving cars.

https://doi.org/10.11003/JPNT.2018.7.1.1